arXiv:1205.3592v1 [nlin.CD] 16 May 2012

Scaling of Energy Spreading in Strongly Nonlinear Lattices

M. Mulansky and A. Pikovsky

Department of Physics and Astronomy, Potsdam University, Karl-Liebknecht-Str 24, D-14476, Potsdam-Golm, Germany

E-mail: `mulansky@uni-potsdam.de`,`pikovsky@uni-potsdam.de`

Abstract. We study scaling properties of energy spreading in disordered strongly nonlinear lattices. Such lattices consist of nonlinearly coupled local linear or nonlinear oscillators, and demonstrate a rather slow, subdiffusive spreading of initially localized wave packets. We use a nonlinear diffusion equation as a heuristic model of this process, and confirm that the scaling predictions resulting from the self-similar solution of this equation are indeed valid for all studied cases. We show that the spreading in nonlinearly coupled linear oscillators slows down compared to a pure power law, while for nonlinear local oscillators a power law is valid in the whole studied range of parameters.

PACS numbers: 05.45.-a, 63.50.-x, 63.70.+h, 05.60.Cd

Submitted to: *NJP*

1. Introduction

Nonlinear Hamiltonian lattices are systems which are easy to formulate and to simulate numerically, but nevertheless their dynamics is far from being fully understood. Generally such a lattice is a non-integrable high-dimensional system demonstrating chaos. So one expects an effective "thermalization" to a statistical equilibrium. However, already the first attempts to follow such a thermalization initiated by Fermi, Pasta, and Ulam revealed many extremely nontrivial effects, still not completely understood (see Refs. [1, 2] for recent progress of the FPU problem). While in the FPU model one is interested in the relaxation to equilibrium from an initial state which is localized in the space of modes (typically one or several modes in a finite lattice are initiated and one follows the transition to an equipartition), recently a problem of a spatial spreading of an initially local in space field has attracted a lot of attention in the studies of nonlinear lattices. Especially nontrivial is such a spreading in the case when linear propagating modes (phonons) do not exist. Then the spreading is due to nonlinear effects only. One way to suppress phonons is to consider lattices with disorder, in this case, due to Anderson localization, linear eigenmodes are exponentially localized and the spectrum is purely discrete. Recent numerical experiments with nonlinear disordered lattices have demonstrated that the initially localized wave packets spread in a very weak, subdiffusive manner [3, 4, 5, 6, 7, 8, 9, 10, 11, 12, 13, 14, 15, 16, 17, 18]. The nontriviality of this observation is that the spreading is due to a weak chaos in the lattice, and it is not clear if this chaos survives when the density of the field becomes very small. All attempts to find the asymptotic properties of this spreading at very large times have been not successful so far, due to numerical problems of following the solutions for very long times.

In this paper we develop the scaling approach to this problem, first suggested in [16]. We will try to establish and to check numerically the scaling properties of spreading, in dependence on the total energy of the initial wave packet. Our guiding tool will be the nonlinear diffusion equation which yields a subdiffusion spreading of a field. We formulate the scaling relations based on this equation, and check their validity for nonlinear lattices.

We will start with formulating the object of our study, strongly nonlinear Hamiltonian lattices. We present a phenomenology of energy spreading and define the statistical quantities characterizing it (Section 2). Next, we introduce a phenomenologic model that we use to describe the properties of the spreading process, namely the Nonlinear Diffusion Equation (NDE) (Section 3). From its self-similar solutions we derive the scaling relations. In Section 4 we present extensive numerical calculations for different types of nonlinearity. These results are compared with the predictions from the NDE. We end with some concluding remarks and outlook.

2. Strongly nonlinear lattices

The main goal of this paper is to study properties of energy spreading in strongly nonlinear lattices. By strongly nonlinear we understand lattices where the coupling is described by nonlinear functions that disappear in the linear limit. So there are no linear waves (phonons) in such lattices and all propagating modes are nonlinear ones. Such lattices can be introduced in the framework of equations for the complex amplitudes (and then one obtains a strongly nonlinear generalization of the nonlinear Schrödinger equation) or as a generalization of a Hamiltonian Klein-Gordon lattice. In this work we follow the latter way. Moreover, we restrict ourselves to pure power-law nonlinearities.

2.1. Hamiltonian

In one dimension we formulated a strongly nonlinear lattice in terms of a Hamilton function for positions q_k and momenta p_k of oscillators labeled by site index k:

$$H = \sum_k \frac{p_k^2}{2} + W\frac{\omega_k^2}{\kappa} q_k^\kappa + \frac{\alpha}{\lambda}(q_{k+1} - q_k)^\lambda \ . \tag{1}$$

Here $\kappa \geq 2$ and $\lambda > 2$ denote the powers of the on-site potential and the coupling term, respectively. For $\kappa = 2$ we have a chain of nonlinearly coupled linear on-site oscillators; for $\kappa > 2$ the on-site oscillators are nonlinear as well. Below we study situations with and without disorder, the latter is introduced via the variations of the parameters of the local potential ω_k (these are linear frequencies of the oscillators if $\kappa = 2$ and parameters of the nonlinear on-site potential if $\kappa > 2$).

2.2. Rescaling

Hamiltonian (1) contains two parameters W and α that determine the time scale and the ratio of local to coupling potentials. For different powers of local and coupling nonlinearities, i.e. for $\kappa \neq \lambda$, we can get rid of these two parameters by rescaling the canonical variables and time as follows:

$$q_k \to W^b \alpha^{-b} q_k \ , \quad p_k \to W^{\lambda b/2} \alpha^{-\kappa b/2} p_k \ , \quad t \to W^{(2-\lambda)b/2} \alpha^{(\kappa-2)b/2} t \ , \tag{2}$$

with $b = 1/(\lambda - \kappa)$. W and α then disappear from the equations and we are left with the total energy $\mathcal{E}$ as the only relevant parameter depending on the initial state. Additionally, a distribution of local "frequencies" ω_k is relevant, while the width of this distribution is rescaled together with W. We will consider three cases: (i) no disorder, $\omega_k = 1$; (ii) "soft" local oscillators, in this case the "frequencies" ω_k are chosen iid. from $[0, 1]$; (iii) "hard" local disorder, here the "frequencies" ω_k are chosen iid. from $[0.5, 1.5]$. In the rescaled coordinates the Hamiltonian reads

$$H = \sum_k \frac{p_k^2}{2} + \frac{\omega_k^2 q_k^\kappa}{\kappa} + \frac{(q_{k+1} - q_k)^\lambda}{\lambda} \ . \tag{3}$$

One special and highly interesting case occurs when the on-site and coupling terms have the same nonlinearity $\kappa = \lambda$. As now all terms containing coordinates q_k have the same power, one cannot set both parameters W and α to one by rescaling as before. Instead, one can use the remaining freedom to set the total energy $\mathcal{E}$ to unity:

$$q \to \mathcal{E}^{1/\kappa} W^{-1/\kappa} q, \quad p \to \mathcal{E}^{1/2} p, \quad t \to W^{-1/\kappa} \mathcal{E}^{1/\kappa - 1/2} \,. \tag{4}$$

Particularly, this means that the energy is not a relevant parameter of the system, but can rather be scaled to, say, $\mathcal{E} = 1$, with a corresponding change of the time scale. Notice that the only remaining parameter is the ratio of strengths of on-site and coupling terms $\beta = \alpha/W$. The rescaled Hamiltonian now reads

$$H = \sum_k \frac{p_k^2}{2} + \frac{\omega_k^2 q_k^\kappa}{\kappa} + \beta \frac{(q_{k+1} - q_k)^\kappa}{\kappa} \,. \tag{5}$$

2.3. Phenomenology of energy spreading

For the Hamiltonian systems (3,5) we state the following question: How does an initially localized field spread over the lattice? We focus on very large systems, where boundary effects are not important. The distribution of the energy is characterized with its density

$$w_k = \frac{E_k}{\mathcal{E}} = \mathcal{E}^{-1} \left(\frac{p_k^2}{2} + W \frac{\omega_k^2}{\kappa} q_k^\kappa + \frac{\alpha}{2\lambda} \left[(q_{k+1} - q_k)^\lambda + (q_k - q_{k-1})^\lambda \right] \right) \,. \tag{6}$$

We start typically with non-zero values of w_k in a small interval (in most runs 10 sites), by choosing initial momenta randomly from a Gaussian distribution, and follow the distribution $w_k(t)$ in time.

In the case of a lattice without disorder, regular waves can propagate along the lattice. Such localized solitary waves – compactons – have been thoroughly studied in [19] for a lattice with $W = 0$ (i.e. without local potential). An initial localized perturbation emits compactons that dominate the process of energy spreading. For $W \neq 0$, it is not known if exact compactons exist in a lattice. In numerics, we quite often observe “quasi-compactons” that propagate ballistically over large distances but lose energy and therefore eventually stop. We illustrate this in Fig. 1(a). In panel (b) we show the same initial conditions in a disordered lattice, here the propagation of “quasi-compactons” is blocked by disorder and one observes a slow spreading of the wave packet. This slow process can be described as follows. At each instance of time, a finite number of oscillators is excited while others have negligible energy. This effectively finite-dimensional Hamiltonian dynamical system demonstrates chaos. Due to this, the next neighbors to the excited region experience a weak chaotic forcing, and their energy slowly grows. After some time their energy reaches the level of the driving neighbor and they become involved into excited, chaotic domain, which in this way increases by one site. This site-by-site propagation means that in disordered, strongly nonlinear lattices at any finite time the distribution of energies is strongly localized, and has sharp edges (we expect that generally the field at the edges decays superexponentially fast, as for breather solutions in such lattices [20]). This sharpness is illustrated in Fig. 2.

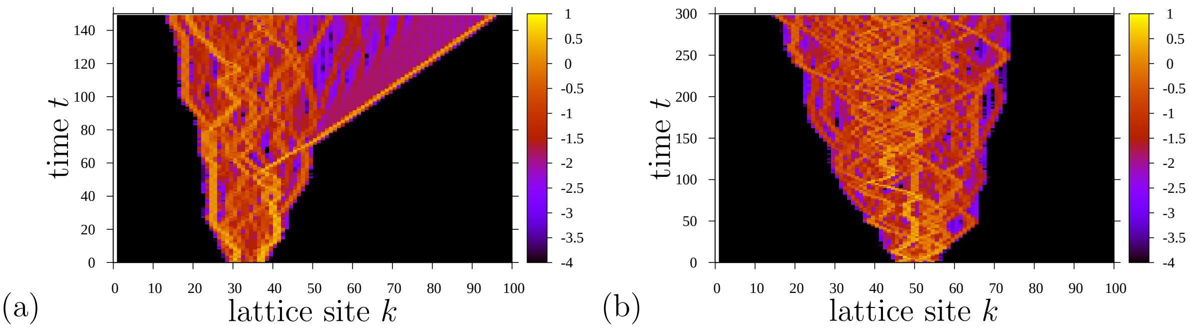

Figure 1. Time evolution of an initially localized state for $\kappa = 4$, $\lambda = 6$, $W = \beta = 1$ and energy $\mathcal{E} = 10$. (a): regular lattice, (b): lattice with "hard" disorder. The color coding corresponds to the logarithm of the local energy excitation $\log_{10} w_k$. The initial excitation was uniform on 10 sites.

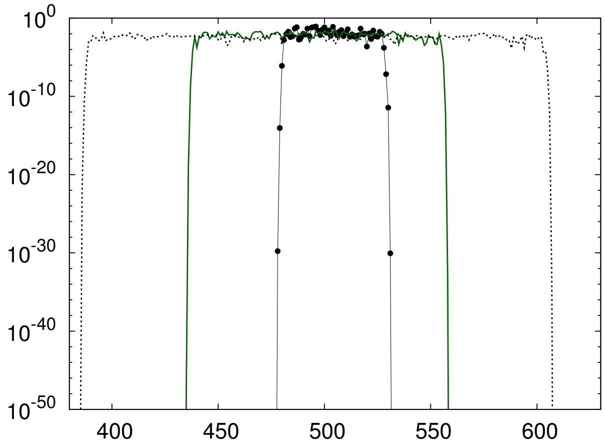

Figure 2. Spreading of an initial single site excitation for $\kappa = 4$, $\lambda = 6$ and energy $\mathcal{E} = 1.0$. The plot shows local energy w_k vs. lattice site k for increasing times 10^4, 10^6, 10^8 (inner to outer curves). Note the logarithmic scaling of w_k and the exponential drops in this scale.

2.4. Measures of spreading

In a statistical context, the spread of a distribution w_k is measured via entropies, most suitable are the Rényi entropies

$$I_q = \frac{1}{1-q} \ln \sum_k w_k^q \,,$$

that allow one to characterize also the spikeness/flatness of the distribution (in the context of energy spreading in disordered lattices this approach was introduced in [14]). We restrict here to the the entropies I_1 and I_2, which are nothing else than the usual Boltzmann entropy and the logarithm of the participation number P:

$$I_1 = -\sum w_k \ln w_k \qquad I_2 = -\ln \sum_k w_k^2 = \ln P \,. \tag{7}$$

The participation number is a characteristic of the width of the wave packet rather popular in the context of Anderson localization studies [14, 8, 21]. Both entropies

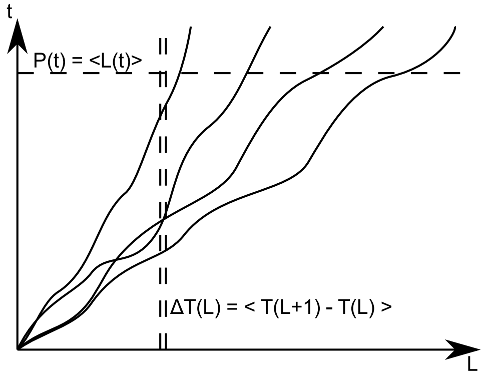

Figure 3. Schematic plot showing the two ways to measure spreading. Averaging at fixed L means averaging at fixed energy density, contrary to averaging at fixed time.

define the effective width of the wave packet as $\mathcal{L}_{1,2} = \exp(I_{1,2})$ (in particular, $\mathcal{L}_2 = P$). As individual dependencies $\mathcal{L}(t)$ demonstrate enormous fluctuations, we perform an averaging of the entropies $I_{1,2}(t)$ over many realizations of disorder, thus obtaining smoothly growing widths $\mathcal{L}(t)$.

For the strongly nonlinear lattices another approach is even superior to the calculation of the entropies. Here we determine the width L of the wave packet as the distance between its sharp edges as seen in Fig. 2 (independently on the distribution of the energy between these edges). After determining the spatial extend L, we measure the time δT required to excite one new lattice site. In other words, $\delta T(L)$ is the time required to pass from L to $L+1$ lattice sites, or the first passage time of the spreading. We define a lattice site as excited when its local energy exceeds some border, in numerics below we take $E_B = 10^{-50}$. The actual value of E_B was chosen arbitrarily, but any other value, e.g. $E_B = 10^{-100}$ would produce similar results. The quantity δT can be interpreted as a propagation time for $L \to L+1$, it can be determined for each particular realization of disorder and initial conditions. After having the ensemble of these propagation times at given L, we calculate the average propagation time ΔT as the geometric average of δT (equivalently, we average the logarithms: $\Delta T = \exp[\langle \log \delta T \rangle]$).

This second approach is superior to the measurement of the effective spatial extent $\mathcal{L}(t)$ for two main reasons:

(i) First, ΔT being the time interval between two spreading events, has no explicit time dependence, hence any prehistory does not appear in later measurements of ΔT. It is therefore easier to compare different realizations and simulations for different parameter values and different initial conditions using ΔT.

(ii) The second advantage relates to the procedure of averaging over many realizations of spreading trajectories. By averaging $\Delta T(L)$ for fixed L, we average over situations with the same energy density $w = \mathcal{E}/L$. If, in contrast, different realizations of $\mathcal{L}(t)$ are averaged for a fixed time t, situations with different energy densities w are averaged together, which is not reasonable if the density w is the crucial parameter on which the properties of the propagation should depend. The difference between averaging

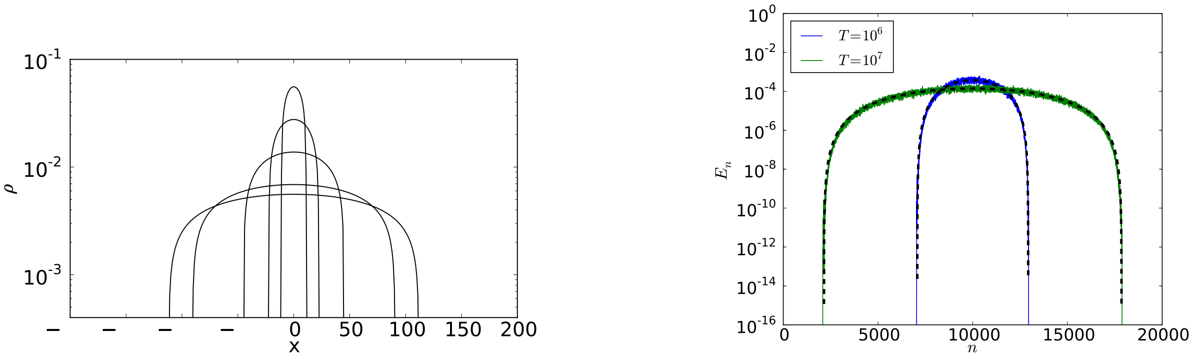

Figure 4. Left: Self similar solution $\rho(x)$ as given by eq. (9) of the NDE for $a = 2$ at times $t = 10^4, 10^5, 10^6, 10^7, 10^8$ (inner to outer lines). Note the logarithmic scaling of ρ. Right: Averaged local energy excitation $\langle E_n \rangle$ of the spreading state in a nonrandom lattice at times $T = 10^6$ and $T = 10^7$ for $\kappa = \lambda = 6$ and $\beta = 4$. The average is taken over $M = 48$ random initial conditions. The dashed black line shows the corresponding analytic self-similar solution of the NDE.

procedures for $\mathcal{L}(t)$ and $\Delta T(L)$ is illustrated in Fig. 3.

3. Nonlinear Diffusion Equation

We study spreading which is induced by nonlinear chaotic interactions between oscillators, it disappears in the linear limit. Phenomenologically, we have seen in Fig. 2 that the spreading looks like a slow diffusion. While we are not able to construct a consistent theory for this process, we will stick to a heuristic approach and use a phenomenologic model to describe the spreading process: the Nonlinear Diffusion Equation (NDE):

$$\frac{\partial \rho}{\partial t} = \frac{\partial}{\partial x}\left(\rho^a \frac{\partial \rho}{\partial x}\right) = \frac{1}{a+1}\frac{\partial^2}{\partial x^2}\rho^{a+1}, \qquad \text{with} \qquad \int \rho \, \mathrm{d}x = \mathcal{E} \; . \tag{8}$$

Here $\rho(x,t)$ is the energy density as a function of position x and time t, and a is a parameter of the nonlinear exponent, which later will be related to the nonlinearities in the lattice models. The second equation represents the energy conservation in this process.

Our main method is to compare the (average) spreading of energy in our lattice model with predictions by the NDE. The NDE has already been successfully applied to nonlinear spreading in the DANSE model [14] and Hamiltonian chains like the ones discussed here [16].

3.1. Self-similar solution

The self-similar solutions of NDE reads [22]

$$\rho(x,t) = \begin{cases} (t-t_0)^{-1/(2+a)} \left(c\,\mathcal{E}^{2a/(a+2)} - \frac{a x^2}{2(a+2)(t-t_0)^{2/(2+a)}} \right)^{1/a} & \text{for} \quad |x| < X \; , \\ 0 & \text{for} \quad |x| > X \; , \end{cases} \tag{9}$$

with c being a constant of integration which follows from the energy conservation:

$$c = \left(\sqrt{\frac{a}{2\pi(a+2)}} \cdot \frac{\Gamma(3/2+1/a)}{\Gamma(1+1/a)} \right)^{2a/(a+2)} .$$

X is the sharp front of the field and has the following time dependence:

$$X = \sqrt{2c\frac{2+a}{a}} \mathcal{E}^{a/(2+a)} (t-t_0)^{1/(2+a)} . \tag{10}$$

The solution has sharp edges (see Fig. 4) and its spatial extension is given by X. The size of the wave packet grows in time as a power law, which can be represented in a scaling form as

$$\frac{X}{\mathcal{E}} \sim \left(\frac{t-t_0}{\mathcal{E}^2} \right)^{1/(2+a)} . \tag{11}$$

In order to get rid of the undetermined time offset t_0, we calculate, following [16], the local inverse velocity of the spreading as $\mathrm{d}t/\mathrm{d}X$ and obtain for it the following scaling law:

$$\frac{1}{X}\frac{\mathrm{d}t}{\mathrm{d}X} \sim \left(\frac{\mathcal{E}}{X} \right)^{-a} . \tag{12}$$

3.2. Implications for spreading in lattices

In our numerical simulations of strongly nonlinear lattices, one approach is to calculate the characteristic size of the wave packet by appropriate averaging of the entropies (7). We can directly associate the size of the field $\mathcal{L}$ with the width of the self-similar solution X, so that in (11) $X \sim \mathcal{L}$. Thus, if we assume that the NDE provides an adequate description of the spreading in strongly nonlinear lattices, the spreading data for different energies should fulfill scaling (11), where the constant a depends generally on the powers κ, λ:

$$\frac{\mathcal{L}}{\mathcal{E}} \sim \left(\frac{t-t_0}{\mathcal{E}^2} \right)^{1/(2+a)} . \tag{13}$$

Similarly, in the second method we calculate the average time ΔT needed for spreading, in dependence of the field spatial extend L (which is equivalent to the size X of the NDE self-similar solution). This quantity directly corresponds to the inverse velocity in (12): $\mathrm{d}t/\mathrm{d}X \sim \Delta T$. Thus, we expect that the times ΔT scale as

$$\frac{\Delta T}{L} \sim \left(\frac{\mathcal{E}}{L} \right)^{-a(w)} . \tag{14}$$

Here we introduced the density w as $w = \mathcal{E}/L$, and have generalized the scaling, allowing for a possible (slow) dependence of the constant a on this density (what will be confirmed by numerics below).

3.3. Scaling for homogeneously nonlinear lattices

In the case of lattices (1) with $\kappa = \lambda$, i.e. when both on-site and coupling nonlinearities have the same power, we can find the relation between the index a and parameter κ analytically. Indeed, from the scaling (4) we obtain that the time scales with energy as

$$t \sim \mathcal{E}^{\frac{2-\kappa}{2\kappa}} \ . \tag{15}$$

Comparing this with the scaling $t - t_0 \sim X^{2+a}\mathcal{E}^{-a}$ we obtain

$$a = \frac{\kappa - 2}{2\kappa} \ , \qquad X \sim (t - t_0)^{\frac{1}{2+a}} \ , \qquad \frac{dt}{dX} \sim X^{1+a} \ . \tag{16}$$

These exact relations will serve as a test for our assumption that the NDE (8) adequately describes the spreading in lattices (1).

4. Numerical Results

In the following sections we report on extensive numerical simulations of strongly nonlinear lattices, trying to check the predictions of the NDE framework. For the numerical time evolution we used a 6th-order symplectic Runge-Kutta scheme [23], mostly with step-size $\Delta t = 0.1$.

4.1. Homogeneous nonlinearity

We start with the case of homogeneous nonlinearity $\kappa = \lambda$, where the scaling index follows from relations (16). The Hamiltonian (5) contains one dimensionless parameter β, additionally the distribution of the local frequencies ω_k should be defined. To test the theoretical predictions (16) we follow the evolution in a one-dimensional lattice with $\omega_k \in [0, 1]$, started from a single site (or several sites for $\kappa = 6$) excitation in the middle. For several values for the nonlinear strength $\beta = 1/4, 1/2, 1, 2$ we we integrated the system up to $T = 10^6$ and analyzed the spreading in terms of $P(t)$ and $\Delta T(L)$. This was repeated for $M = 100$ realizations of disorder. Fig. 5 shows the averaged results of these runs for the excitation time $\Delta T(L)$ for $\kappa = 4$ (left panel) and $\kappa = 6$ (right panel). In both cases we find a quite nice agreement of the numerical results with the analytic predictions of the NDE (16). We also performed simulations choosing the disorder to be $\omega_k \in [0.5, 1.5]$ and got similar results (not presented here). Additionally, results for the direct spreading measure $P(t)$ show the same agreement with prediction (16) (see ref. [16]). To our opinion, the agreement between numerics and prediction is a rather convincing evidence that the NDE provides the proper framework to model the average energy spreading in nonlinear Hamiltonian chains.

Remarkably, the NDE scaling (16) holds also for one-dimensional lattices without disorder. Fig. 6 shows the participation number evolution for lattice (5) with $\omega_k = 1$ and $\kappa = 4, 6$. In this case the excitation times ΔT are not the proper measures as they are dominated by quasi-compactons (cf. Fig. 1(a)), but the participation number calculations are insensitive to such modes. For them we expect from (16) the scaling

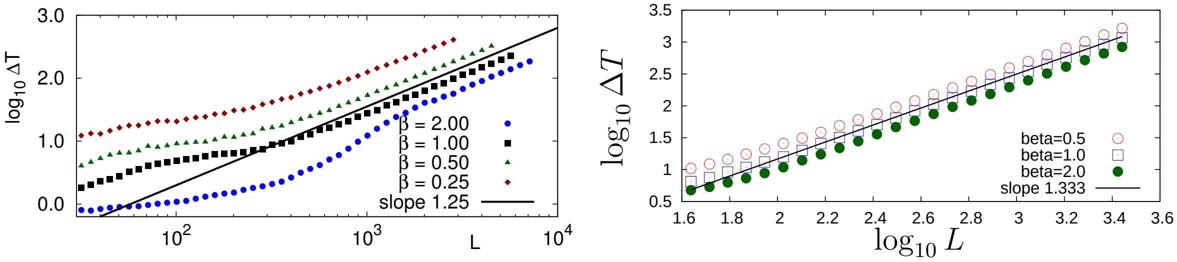

Figure 5. Excitation times ΔT for the lattices with homogeneous nonlinearities, $\kappa = \lambda = 4$ (left panels) and $\kappa = \lambda = 6$ (right panels). The black lines show the predicted behaviors [see (16)] $\Delta T \sim L^{5/4}$ (left) and $\Delta T \sim L^{4/3}$ (right) respectively.

$P \sim (t - t_0)^{\frac{2\kappa}{5\kappa-2}}$ which is confirmed in Fig. 6. This is also supported by the direct comparison of spreading states from the numerical simulation to the self similar solution, as can be seen in right panel of Fig. 4.

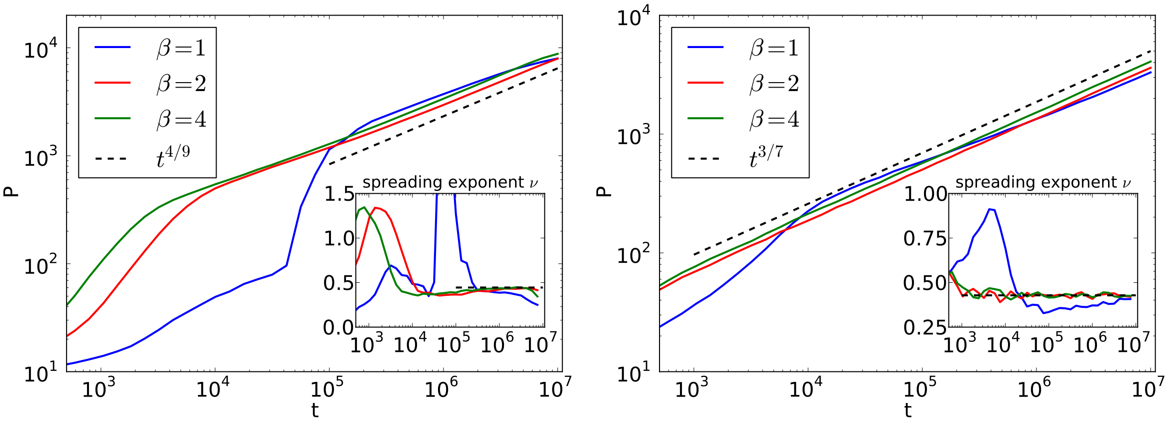

Figure 6. Participation number for a nonrandom lattice with $\kappa = \lambda = 4$ (left panel) and $\kappa = \lambda = 6$ (right panel) averaged over $M = 48$ random initial conditions (solid lines). The dashed lines shows the NDE prediction $P \sim t^{4/9}$ and $P \sim t^{3/7}$ respectively. In the inset we plot the numerical spreading exponent ν obtained from finite differences of the method above, the dashed line there also corresponds to the expectation from the NDE. Notice that a slight final deviation of the spreading exponent for $\beta = 1, 2$ in the inset of Fig. 6 is due to boundary effects as we hit the maximum lattice size at the end of integration.

4.2. Linear on-site Potential, Nonlinear Coupling

After having found that the NDE provides a good description of the spreading for the case of homogeneous nonlinearity, we turn now to a general situation with $\kappa \neq \lambda$. In this section we assume the on-site potential to be quadratic $\kappa = 2$, for the coupling we chose $\lambda = 4$ and $\lambda = 6$. This is the case of nonlinearly coupled linear oscillators. It corresponds to a rather general situation of nonlinear disordered lattices, where in the representation of linear eigenmodes one can also interprete the system as an ensemble of nonlinearly coupled linear modes. The main difference of our setup of strongly nonlinear

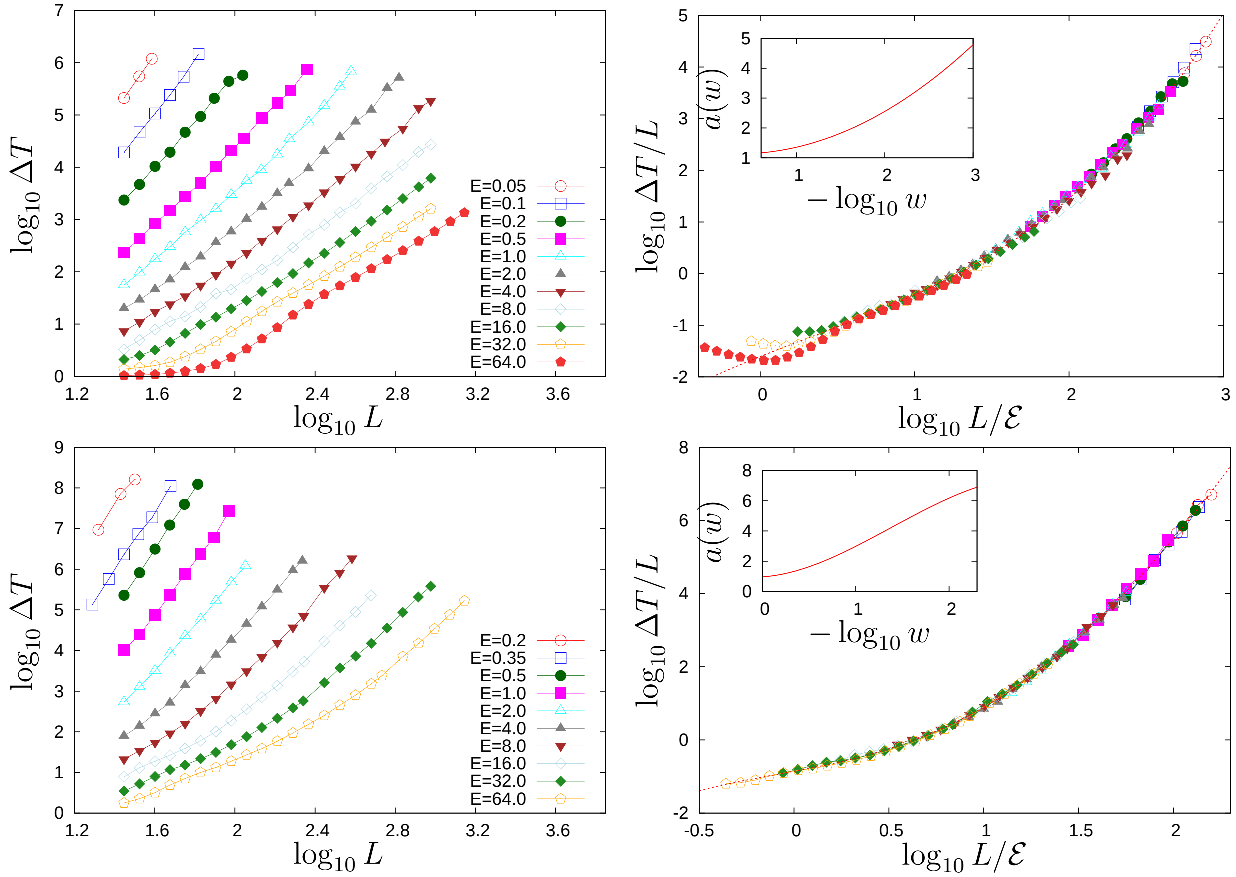

Figure 7. Excitation times $\Delta T(L)$ for the case with linear on-site term and nonlinear coupling $\kappa = 2$, $\lambda = 4$. The upper panels show results for disorder chosen as $\omega_k = [0, 1]$ while in the lower two graphs we had $\omega_k = [0.5, 1.5]$. In the left panels you see direct results $\Delta T(L)$ while on the right the scaling from the NDE has been applied and we plot $\Delta T/L$ vs. $L/\mathcal{E}$. Each color/symbol belongs to an averaged value over disorder realization for a fixed energy $\mathcal{E}$. The inlets on right panels show dependence of the nonlinearity index $a(w)$ on the density w, obtained via polynomial fitting of the data (dashed red lines).

lattices from that of coupled linear modes, is that here the linear oscillators interact only with the nearest neighbors, and the interaction terms contain no disorder, while in general lattices, the modes interact with several other modes and the interaction terms are disordered, because the coupling involves the overlap of the exponentially localized, disordered eigenmodes.

As outlined in section 2.2, the only free parameter in the Hamiltonian (3) is the conserved energy $\mathcal{E}$, and we analyze the excitation times $\Delta T(L)$ as function of the wave packet length L, for different energies $\mathcal{E}$. Our goal is to check the predictions of the NDE scaling (14).

In Fig. 7 we report the results for $\kappa = 2$ and $\lambda = 4$. We have performed many runs for different realizations of disorder choosing $\omega_k \in [0, 1]$ and $\omega_k \in [0.5, 1.5]$, and for different total energies (some of these results have already been presented in [16]). For each disorder realization, several sites are initially excited, and from the evolution of the field the propagation times $\Delta T(L)$ were determined as described in section 2.4. Left panels of Fig. 7 show these times in dependence on L for different energies. Applying the energy scaling according to (14), however, we find a perfect collapse to a single curve for all energy values, as demonstrated in right panels of Fig. 7. The same collapse of data can be observed in Fig. 8 for $\kappa = 2$, $\lambda = 6$, where we only show the rescaled plots.

Hence, we found that for both cases $\lambda = 4, 6$ and the two disorder ranges $[0, 1]$, $[0.5, 1.5]$, the energy scaling resulting from the NDE is valid over more than two orders of magnitude of the total energy $\mathcal{E}$. However, from the scaled plots one can see that the resulting graph is not a straight line with slope a as predicted by the NDE, but a curved one. This means that the nonlinearity index a is effectively density dependent, so we define

$$a(w) = -\frac{d}{dw}\left(\frac{\Delta T}{L}\right)$$

and show this values in the inlets. The curves bend upwards and hence $a(w)$ increases with decreasing energy density (note that the x-axis in Figs. 7 and 8 represent $L/\mathcal{E} = w^{-1}$) resulting in longer excitation times and slower spreading for smaller densities.

We conclude that in the case $\kappa = 2$, $\lambda = 4, 6$ we find the NDE to give an adequate description in the sense of correct energy scaling. However, numerical results here indicate that the nonlinearity parameter in the NDE is (logarithmically) density dependent $a(w)$, and increases with decreasing density. As the density decreases in course of the excitation spreading, this also results in a decrease of the effective spreading exponent $(2+a)^{-1}$ with time. The question of the asymptotic behavior remains, however, open: from the data presented we cannot judge whether the spreading effectively stops, or continues with an increasing index a, or some transition to another law of spreading (e.g., a logarithmic one) occurs.

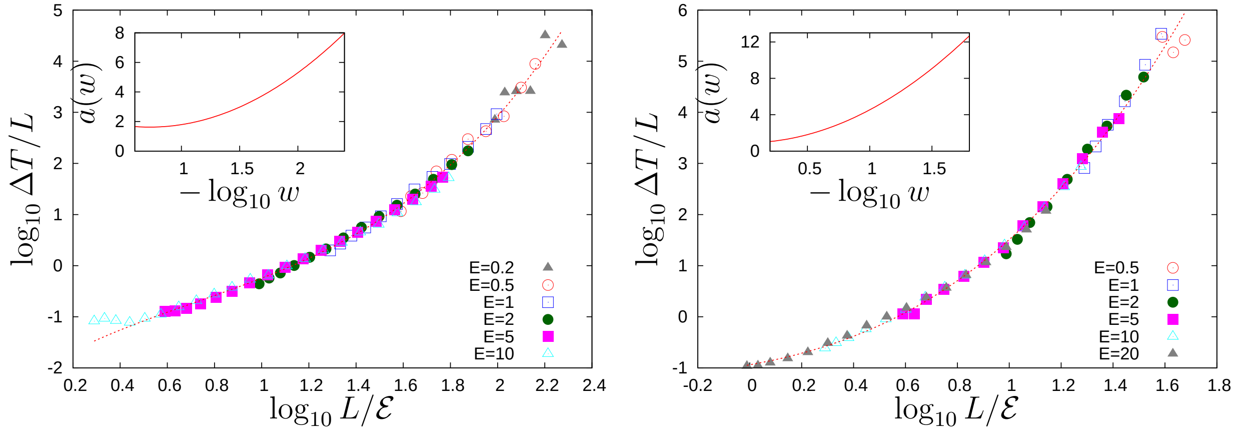

Figure 8. Scaled excitation times $\Delta T(L)$ for the lattice with linear on-site term and nonlinear coupling $\kappa = 2$, $\lambda = 6$. In the left panels you see the scaled results $\Delta T/L$ vs. $L/\mathcal{E}$ for $\omega_k \in [0, 1]$ while on the right we set $\omega_k \in [0.5, 1.5]$. Each color/symbol belongs to an averaged value over disorder realization for a fixed energy. The inlets show the density dependencies $a(w)$ obtained through the cubic approximation of the data points (dashed red curves).

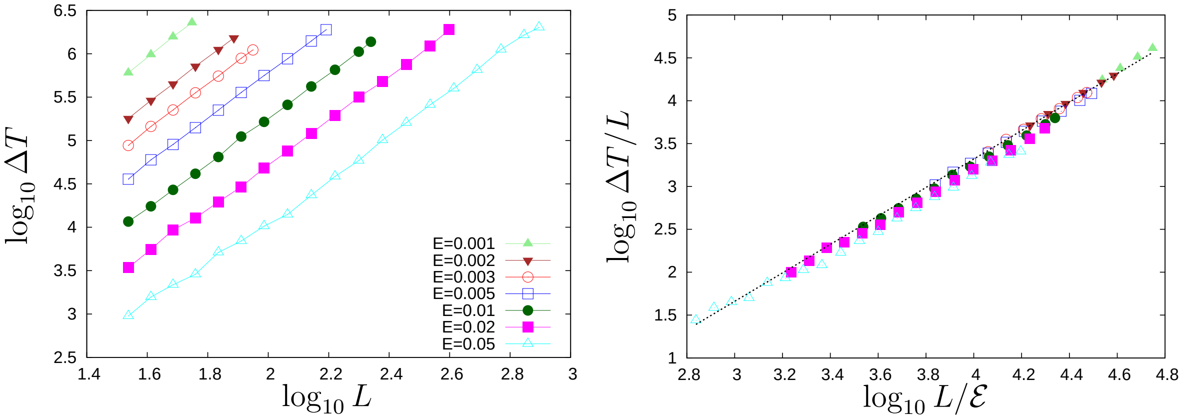

Figure 9. Excitation times $\Delta T(L)$ for $\kappa = 4$, $\lambda = 6$ with energies $\mathcal{E} = 0.001 \ldots 0.05$. The left panel shows the original data while on the right panel scaled variables as suggested by the NDE are used: $\Delta T/L$ vs. $L/\mathcal{E}$. The dashed black line has slope 1.66.

4.3. Nonlinear on-site Potential, Nonlinear Coupling

In this section we describe the lattice with $\lambda = 4$ and $\kappa = 6$, i.e. a lattice of nonlinearly coupled nonlinear on-site oscillators. In this case, the disorder parameter ω_k in (3) does not have the meaning of an oscillator frequency, but is the coefficient determining the nonlinearity strength. The real frequency of oscillations depends on the local energy at the site. In Fig. 1 we show an exemplary time evolution of an initially localized state in such a lattice.

Again, we investigate the excitation times $\Delta T(L)$ for different total energies in the same way as above. Results of our simulations for $\omega_k \in [0.5, 1.5]$ are shown in Fig. 9. In the right panel the scaling as suggested by the NDE (14) is applied. We again find a perfect overlapping of the numerical curves supporting the validity of the NDE. Contrary to the previous result for nonlinear coupled linear oscillators ($\kappa = 2$), we find that data of the right panel of Fig. 9 can be nicely fitted with a straight line. This means that the parameter a does not dependent on the density. Hence, in this case the NDE gives not only the correct scaling, but can be also applied in the standard form with a constant effective parameter a. The results in Fig. 9 show roughly $\Delta T/L \sim (L/\mathcal{E})^{1.66}$ which means, according to (12), $a \approx \frac{5}{3}$. This gives for the participation number the subdiffusive spreading $P \sim t^{3/11}$. In Fig. 10 we check this by directly analyzing $P(t)$ for different energies. As one can see in the right panel, the scaling predicted from the NDE (11) works rather well for an enormous range of energy values $\mathcal{E} = 0.001 \ldots 1$. The scaling is not as perfect as for the excitation times above, which we believe comes from the fact that the excitation times are better representatives of the spreading behavior in this system as discussed in section 2.4 (and, additionally, no fitting of the time offset t_0 has been performed). The asymptotic slope of the scaled curve is in a good accordance with the results for the excitation times in Fig. 9.

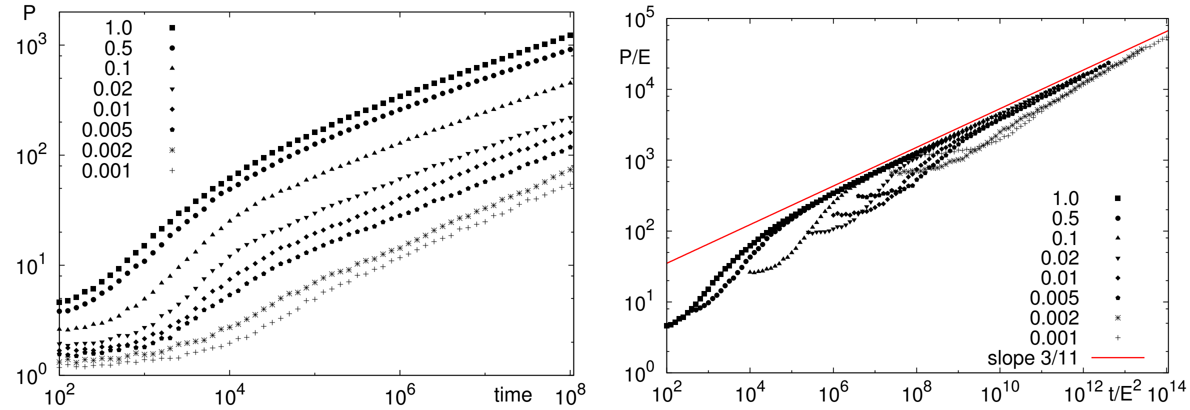

Figure 10. Participation Number $P(t)$ for $\kappa = 4$, $\lambda = 6$ and energies $\mathcal{E} = 0.001 \ldots 1$. The left panel shows original data while on the right the scaling variables $P/\mathcal{E}$ vs. $t/\mathcal{E}^2$ are shown. The slope of the red line is $3/11$ which corresponds to $a = 5/3$ as found in Fig. 9 above.

5. Conclusions

Motivated by previous observations of subdiffusive behavior in nonlinear disordered systems, we used the Nonlinear Diffusion Equation as a phenomenologic model to describe the spreading process in disordered one-dimensional Hamiltonian lattices of nonlinearly coupled oscillators. We have found that the NDE not only predicts a subdiffusive spreading, but also induces a one-parameter scaling of time and energy of the spreading process according to relations (13,14). We tested these scaling laws on a class of nonlinearly coupled oscillators with different values of the nonlinear exponents κ and λ. In all considered cases the one-parameter scaling laws were nicely reproduced in our numerical study. In this sense one can say that the spreading in nonlinear disordered one-dimensional lattices belongs to a “universality class” of NDE. For nonlinearly coupled linear disordered oscillators, we have found a remarkable dependence of the effective index of nonlinearity of NDE on the energy density. As the effective nonlinearity increases in the course of spreading, this means a slowing down of the spreading process compared with the perfect power law. Still, it is not possible to judge from the data, what is the asymptotic regime of the spreading.

The essential step of our study is an introduction of a novel quantity, characterizing the spreading – the averaged excitation time ΔT. This quantity, defined as a first passage time for a particular size of the wave packet, and thus for a particular value of the density, allows us to reveal the density dependence of the spreading characteristics, what is hardly possible with old approaches where, e.g., the averaged participation numbers have been followed (cf. a clear scaling in Fig. 9 with a weakly converging asymptotic in Fig. 10). Unfortunately, the calculation of the averaged excitation time is relied on the sharp edges of the field, so its application to linearly coupled lattices where eigenmodes are exponentially (but not sharp) localized, remains a challenge for future studies. Also, in future studies it would be desirable to extend the analysis to two-dimensional lattices.

Acknowledgement

The numerical results have been partially obtained at the CINECA sp6 supercomputer under the Project HPC-EUROPA2 (Project number 228398), with the support of the European Community - under the FP7 “Research Infrastructure” Programme.

References

[1] G. Gallavotti, editor. *The Fermi-Pasta-Ulam problem.* Springer Lecture Notes in Physics vol. 728, 2008.

[2] A focus issue on “The “Fermi-Pasta-Ulam” problem – the first 50 years” (ed. by D. K. Campbell, P. Rosenau and G. Zaslavsky). *CHAOS*, 15(1), 2005.

[3] D. Shepelyansky. Delocalization of quantum chaos by weak nonlinearity. *Phys. Rev. Lett.*, 70:1787–1790, 1993.

[4] M. I. Molina. Transport of localized and extended excitations in a nonlinear Anderson model. *Phys. Rev. B*, 58(19):12547–12550, 1998.

[5] A. S. Pikovsky and D. L. Shepelyansky. Destruction of Anderson localization by a weak nonlinearity. *Phys. Rev. Lett.*, 100(9):094101, 2008.

[6] S. Fishman, Y. Krivolapov, and A. Soffer. On the problem of dynamical localization in the nonlinear Schrodinger equation with a random potential. *J. Stat. Phys.*, 131(5):843–865, 2008.

[7] I. Garcia-Mata and D. L. Shepelyansky. Nonlinear delocalization on disordered Stark ladder. *Eur. Phys. J. B*, 71(1):121–124, 2009.

[8] S. Flach, D. O. Krimer, and Ch. Skokos. Universal spreading of wave packets in disordered nonlinear systems. *Phys. Rev. Lett.*, 102(2):024101, 2009.

[9] Ch. Skokos, D. O. Krimer, S. Komineas, and S. Flach. Delocalization of wave packets in disordered nonlinear chains. *Phys. Rev. E*, 79(5, Part 2):056211, 2009.

[10] M. Mulansky, K. Ahnert, A. Pikovsky, and D. L. Shepelyansky. Dynamical thermalization of disordered nonlinear lattices. *Phys. Rev. E*, 80:056212, 2009.

[11] Ch.Skokos and S. Flach. Spreading of wave packets in disordered systems with tunable nonlinearity. *Phys. Rev. E*, 82(1):016208, 2010.

[12] S. Flach. Spreading of waves in nonlinear disordered media. *Chem. Physics*, 375(2-3):548–556, OCT 5 2010.

[13] T. V. Laptyeva, J. D. Bodyfelt, D. O. Krimer, Ch.Skokos, and S. Flach. The crossover from strong to weak chaos for nonlinear waves in disordered systems. *Europhys. Lett.*, 91(3):30001, 2010.

[14] M. Mulansky and A. Pikovsky. Spreading in disordered lattices with different nonlinearities. *Europhys. Lett.*, 90:10015, 2010.

[15] M. Johansson, G. Kopidakis, and S. Aubry. KAM tori in 1D random discrete nonlinear Schrödinger model? *Europhys. Lett.*, 91(5):50001, 2010.

[16] M. Mulansky, K. Ahnert, and A. Pikovsky. Scaling of energy spreading in strongly nonlinear disordered lattices. *Phys. Rev. E*, 83:026205, 2011.

[17] M. V. Ivanchenko, T. V. Laptyeva, and S. Flach. Anderson localization or nonlinear wave? A matter of probability. *Phys. Rev. Lett.*, 107:240602, 2011.

[18] S. Fishman, Y. Krivolapov, and A. Soffer. The nonlinear Schrödinger equation with a random potential: results and puzzles. *Nonlinearity*, 25(4):R53–R72, 2012.

[19] K. Ahnert and A. Pikovsky. Compactons and chaos in strongly nonlinear lattices. *Phys. Rev. E*, 79:026209, 2009.

[20] P. Rosenau and S. Schochet. Almost compact breathers in anharmonic lattices near the continuum limit. *Phys. Rev. Lett.*, 94(4):045503, 2005.

[21] H. Veksler, Y. Krivolapov, and S. Fishman. Spreading for the generalized nonlinear Schrödinger equation with disorder. *Phys. Rev. E*, 80(3):037201, 2009.

[22] A. D. Polyanin and V. F. Zaitsev. *Handbook of Nonlinear Partial Differential Equations.* Chapman & Hall, 2003.

[23] R. I. McLachlan. On the numerical integration of ordinary differential equations by symmetric composition methods. *SIAM J. Sci. Computing*, 16(1):151–168, 1995.